

Reduction of Activated Olefins by SmI_2 . Detouring the Classical Birch Mechanism and a Negative Order in SmI_2

Alexander Tarnopolsky and Shmaryahu Hoz*

Contribution from the Department of Chemistry, Bar-Ilan University, Ramat-Gan 52900, Israel

Received December 4, 2006; E-mail: shoz@mail.biu.ac.il

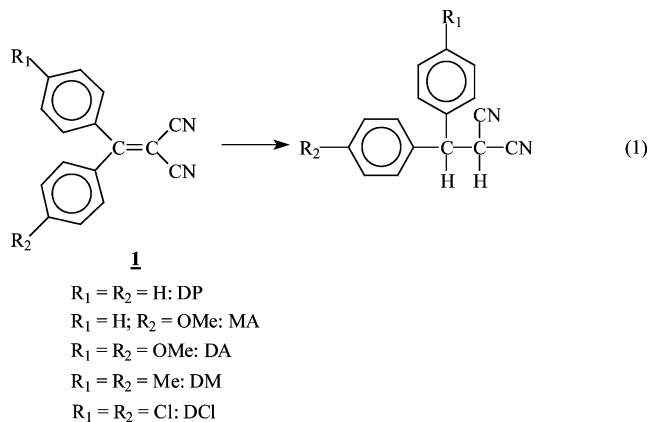
Abstract: The reaction of an excess of 1,1-diaryl-2,2-dicyanoethylenes (**1**) with SmI_2 is biphasic for olefin with at least one available para position. The first phase is completed in less than 0.5 s with the second phase extending over a few hundred seconds. This phase is second order with respect to the radical anion, which is formed in the dead-time of the mixing in the stopped flow spectrophotometer and is overall of -1 order in the initial concentration of SmI_2 . In this phase, a dimer is formed between two radical anions with the formation of a C–C bond between a benzylic and a para position. The second phase is enhanced by proton donors and shows an H/D kinetic isotope effect with MeOH. Minute amounts of ethylene glycol accelerated the reaction to such an extent that the second phase is “absorbed” into the first, rendering it rate determining. In this phase, the dianionic dimer disproportionates after protonation to furnish the neutral species and the anion, which after second protonation provides the reduced product. When the two para positions are occupied by substituents, the reaction takes place by the traditional Birch reduction sequence of electron–proton–electron–proton–transfer steps. It is shown that the detour mechanism, coupling followed by disproportionation, should be typical of olefin but not of carbonyl reduction. This difference stems from the dissimilarity in protonation rate on carbon and oxygen.

Introduction

Since its introduction by Kagan¹ in 1977, SmI_2 has become one of the most popular reagents in single electron-transfer-based synthetic chemistry. Research efforts in recent years focused on additives that facilitate the reaction as well as on the study of the intimate details of the reaction of SmI_2 with various substrates and functional groups.² Surprisingly, very little has been done to advance our understanding of the reduction of carbon–carbon double bonds.³ This paper reports that the reduction of C=C bonds by SmI_2 to produce the hydrogenated compound takes a route entirely different from the traditional Birch reduction sequence⁴ of electron–proton–electron–proton–

transfer steps. Moreover, this study suggests that, in many cases, the reduction mechanism of C=C bonds will differ from the reduction of the corresponding C=O bonds by SmI_2 .

Specifically, we have studied the reaction shown in eq 1 and discovered that when mono- or unsubstituted 1,1-diaryl-2,2-dicyanoethylenes (**1**) react with SmI_2 , they display a mechanism entirely different from that of the disubstituted substrates, although affording the same type of final product (**2**) in a quantitative yield.



Results and Discussion

To simplify the kinetics of the reaction, the reduction of **1** was performed with substrates in a large excess over SmI_2 . The

- (1) Namy, J. L.; Girard, P.; Kagan, H. B. *New J. Chem.* **1977**, *1*, 5–7. For some recent reviews, see: (a) Edmonds, D. J.; Johnston, D.; Procter, D. J. *Chem. Rev.* **2004**, *104*, 3371–3403. (b) Kagan, H. B. *Tetrahedron* **2003**, *59*, 10351–10372. (c) Steel, P. G. *J. Chem. Soc., Perkin Trans. 1* **2001**, 2727–2751. (d) Krief, A.; Laval, A.-M. *Chem. Rev.* **1999**, *99*, 745–777. (e) Molander, G. A.; Harris, C. R. *Tetrahedron* **1998**, *54*, 3321–3354. (f) Molander, G. A.; Harris, C. R. *Chem. Rev.* **1996**, *96*, 307–338.
- (2) (a) Enemaerke, R. J.; Hertz, T.; Skrydstrup, T.; Daasbjerg, K. *Chem.-Eur. J.* **2000**, *6*, 3747–3754. (b) Prasad, E.; Knettle, B. W.; Flowers, R. A., II. *J. Am. Chem. Soc.* **2004**, *126*, 6891–6894. (c) Molander, G. A.; McKie, J. A. *J. Org. Chem.* **1992**, *57*, 3132–3139. (d) Pedersen, H. L.; Christensen, T. B.; Enemaerke, R. J.; Daasbjerg, K.; Skrydstrup, T. *Eur. J. Org. Chem.* **1999**, 565–572. (e) Hutton, T. K.; Muir, K. W.; Procter, D. J. *Org. Lett.* **2003**, *5*, 4811–4814. (f) Imamoto, T.; Takeyama, T.; Yokoyama, M. *Tetrahedron Lett.* **1984**, *25*, 3225–3226. (g) Imamoto, T.; Hatajima, T.; Takiyama, N.; Takeyama, T.; Kamiya, Y.; Yoshizawa, T. *J. Chem. Soc., Perkin Trans. 1* **1991**, 3127–3135. (h) Chopade, P. R.; Prasad, E.; Flowers, R. A. *J. Am. Chem. Soc.* **2004**, *126*, 44–45. (i) Dahlen, A.; Hilmersson, G.; Knettle, B. W.; Flowers, R. A., II. *J. Org. Chem.* **2003**, *68*, 4870–4875. (j) Dahlen, A.; Nilsson, A.; Hilmersson, G. *J. Org. Chem.* **2006**, *71*, 1576–1580. (k) Hasegawa, E.; Curran, D. P. *J. Org. Chem.* **1993**, *58*, 5008–5010. (l) Prasad, E.; Flowers, R. A., II. *J. Am. Chem. Soc.* **2005**, *127*, 18093–18099.
- (3) (a) Yacovan, A.; Bilkis, I.; Hoz, S. *J. Am. Chem. Soc.* **1996**, *118*, 261–262. (b) Yacovan, A.; Hoz, S. *J. Org. Chem.* **1997**, *62*, 771–772.

- (4) Allinger, N. L.; Cava, M. p.; DeJonj, D.; Johnson, C. R.; Lebel, N. A.; Stevens, C. L. *Organic Chemistry*; Worth Publishing: New York, 1973; p 382.

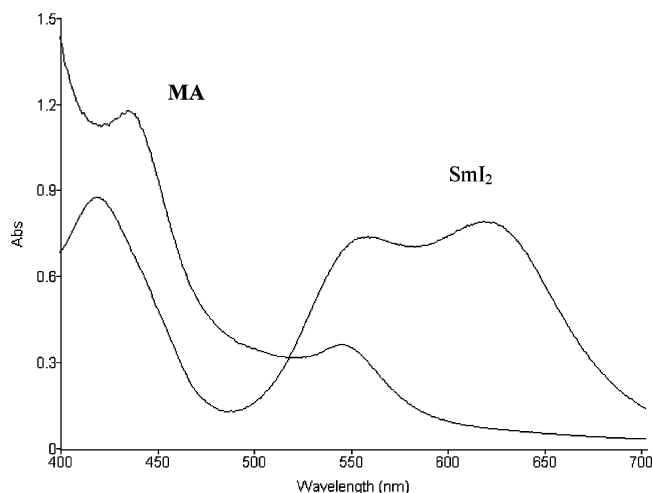


Figure 1. Spectra of the radical anion of **MA** (1.5 mM) and SmI_2 (9 mM) in THF.

rates of reaction were monitored using stopped flow spectroscopy. Upon mixing the THF solutions of the SmI_2 and the substrate, the spectrum of SmI_2 vanishes completely and the radical anion of the substrate is quantitatively and immediately obtained (within the “dead-time” of the mixing). This species is characterized by two distinct absorptions around 430 and 550 nm. Figure 1 shows the spectrum of the radical anion of **MA**.⁵

DP and **MA** display the following unexpected features: (a) The reaction is biphasic with the first phase completed in less than 0.5 s and the second phase extending over a few hundred seconds. (b) The first phase is second order in the initially formed radical anion. (c) A plot of $\log k$ of the first phase versus the log of the initial concentration of SmI_2 shows a negative order (-1). (d) The first phase is insensitive to the presence of proton donors. Yet, they greatly enhance the second phase. At a high proton donor concentration, the reaction is accelerated to such an extent that the second phase is “absorbed” in the first phase, rendering it rate determining. (e) The H/D kinetic isotope effect for the second phase with MeOH reaches the value of 2.7, and the kinetic order in MeOH varies from 0.3 to 1 as MeOH concentration increases. The reaction of **DP** and **MA** (substrates having at least one unsubstituted phenyl group) is biphasic (see Figure S1). The two phases will be discussed separately below.

Substrates substituted at both para positions display an entirely different behavior, and their reaction times are in the range of hundreds of seconds.

Nature of the First Phase. The disappearance of the absorptions of the radical anion showed a perfect fit to a second-order reaction in the radical anion. Quenching the reaction mixture after the first phase showed this not to be the product-forming step. Even after 60 s, only 34% of the reduced product was formed. The bimolecular nature of this phase may correspond either to a disproportionation forming a dianion or to a dimer formation. The first possibility could be safely ruled out on the basis that the reaction of substrates that are disubstituted by electron-donating (**DA** = para di-MeO, **DM** = para di-Me) or by electron-attracting (**DCI** = para di-Cl) substituents is slower by ca. 3 orders of magnitude than that of

Scheme 1

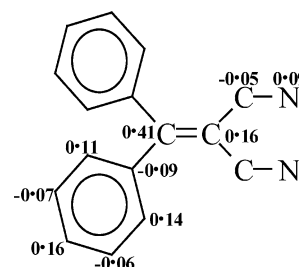
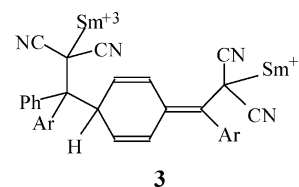


Table 1. Effect of Variable Concentrations of $[\text{SmI}_2]_0$ on the Second-Order Rate Constant of **DP** (25 mM)

$[\text{SmI}_2]$ (mM)	k_{obs} ($\text{M}^{-1} \text{s}^{-1}$)
1.5	10 000
3	6700
4.4	4700
6	2700

the mono- or unsubstituted substrates. Dimerization seems, therefore, to be the preferred option. Ab initio calculations (computations were performed at the B3LYP/6-31+G* level using the Gaussian 03 code⁶) show that, in the unsubstituted radical anion, high spin density (0.41) is concentrated on the benzylic carbon (Scheme 1).

Thus, on the basis of spin density, a pinacol-type coupling is expected with bonding between the two benzylic positions. However, this mode of dimerization is unlikely because of the large steric hindrance. The difference in the reactivity pattern between the disubstituted and the mono- or unsubstituted substrates suggests that the para position is involved in the dimerization. Indeed, the spin density at the para position is also relatively high (0.16), suggesting dimerization through this position. Coupling between two para positions, which encompasses a loss of aromaticity of two rings, is less likely than a benzylic–para position bond formation (**3**).



3

We assume, therefore, that the dimer has the structure **3**, which finds precedent in other systems.⁷

The rate constant for the dimerization of the radical anion of **DP** ($[\text{DP}] = 5\text{--}12.5$ mM; $[\text{SmI}_2] = 1.25$ mM) is $10\,750 \pm 450 \text{ M}^{-1} \text{ s}^{-1}$, and for the dimerization of the radical anion of **MA** ($[\text{MA}] = 6.5\text{--}25$ mM; $[\text{SmI}_2] = 1.5$ mM) it is $5670 \pm 290 \text{ M}^{-1} \text{ s}^{-1}$. The lower rate constant for **MA** probably reflects the statistical factor for coupling at the para position.

One of the most interesting results obtained in this study is the negative order (-1) found in the initial concentration of the SmI_2 . As can be seen from Table 1 and Figure 2 (for **MA**, see Table S1), the second-order rate constant decreases as the initial concentration of SmI_2 increases.

(5) A similar spectrum was obtained upon mixing a solution of the substrate with a solution of Na/benzophenone in THF. The absorptions in this case were slightly shifted to longer wavelengths, 460 and 580 nm.

(6) Frisch, M. J.; et al. (for complete reference, see Supporting Information).
(7) Shiue, J.-S.; Lin, C.-C.; Fang, J.-M. *Tetrahedron Lett.* **1993**, *34*, 335–338.

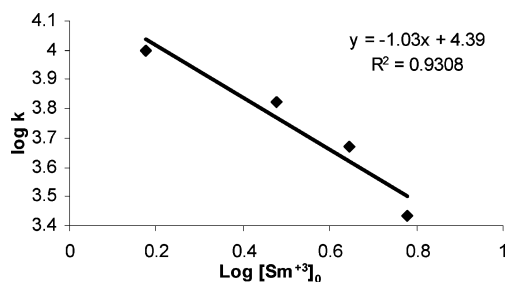


Figure 2. A plot of the effect of different initial SmI_2 concentrations on the second order of the first phase for the reaction of **DP** (25 mM).

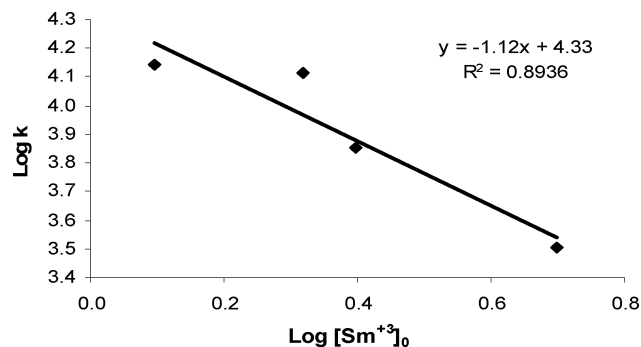


Figure 3. A plot of the effect of the total Sm^{+3} concentration on the second-order rate constants of the first phase for the reaction of **DP** (12.5 mM) and SmI_2 (1.25 mM).

Table 2. Effect of the Added Sm^{+3} on the Second-Order Rate Constants of the First Phase for the Reaction of **DP** (12.5 mM) and SmI_2 (1.25 mM)

$[\text{Sm}^{+3}]$ (mM)	k_{obs} ($\text{M}^{-1} \text{s}^{-1}$)
0	14 000
0.83	13 000
1.25	7100
3.75	3200

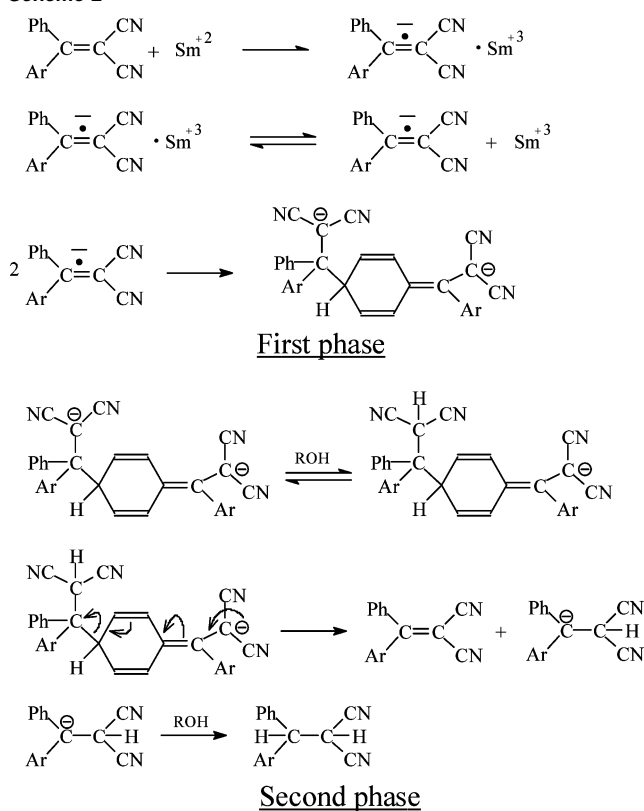
It should be emphasized that the rate of the reaction increases with the increase in the initial concentration of the SmI_2 . However, doubling the initial concentration of SmI_2 doubles the concentration of the radical anion, and, due to the bimolecular nature of the reaction, the rate should increase by 4-fold. Thus, a 2-fold increase in the rate corresponds to the observed negative order.

This behavior is typical for the presence of an inhibitor introduced to the reaction mixture at its beginning. Because the reactions show a very good fit, within a run, to a second-order reaction, it implies that the concentration of the inhibitor is constant during the reaction time. Upon mixing of the reactants, two new species are produced, the radical anion and Sm^{+3} . However, only the concentration of Sm^{+3} remains constant, and, therefore, Sm^{+3} is likely to be the inhibitor. To confirm this conclusion, we have generated in situ variable amounts of Sm^{+3} by titrating with I_2 an excess of SmI_2 initially introduced into the reaction mixture. Results shown in Table 2 and Figure 3 (for **MA**, see Table S2) clearly demonstrate the inhibitive nature of Sm^{+3} .⁸

A conceivable inhibition mechanism follows. Comparing the reduction potential of **DP** and oxidation potential of SmI_2 , it is

(8) In this case, the rate constants decrease because the increase in the Sm^{+3} concentration is not accompanied by an increase in the radical anion concentration.

Scheme 2



clear that the reduction process is highly endothermic.⁹ The change from an endothermic to an exothermic process is due to the Coulombic interaction energy gained by the ion pairing of the Sm^{+3} and the radical anion.

However, the large samarium cation with its solvation sphere and possibly also with one or two iodide ions in its vicinity may sterically inhibit the dimerization. Dimerization can therefore take place mainly with the “free” radical anion. If the ion pairing equilibrium is significantly tilted toward the paired ions, and dimerization takes place from the minute amount of the free radical anion, then the inhibition will be linearly proportional to the concentration of the inhibitor (Sm^{+3}) as we have observed.¹⁰ A possible additional cause for the inhibition could be that the counterion changes the spin distribution in the radical anion (Scheme 1) in such a way that largely reduces the likelihood of dimerization (reducing the product of the spin densities on the bond forming carbon atoms).

Thus, the suggested reaction mechanism (Scheme 2) seems to adequately accommodate all of the observed phenomena of the first phase. We go next to the second phase.

Nature of the Second Phase. The kinetics of this phase is insensitive (zero order) to variations in the initial concentrations of the substrate and the SmI_2 . It is first order in the dimer and of varying order in the added MeOH. While the dimer absorption vanishes only after several hundred seconds in the absence of a proton donor, in the presence of 1.25 M MeOH, 35% of the product was already obtained after 1 s. The rate

(9) The reduction potential of **DP** in THF vs SCE is -1.08 V (ref 3a), whereas that of SmI_2 is -0.9 V (Enemærke, R. J.; Daasbjerg, K.; Skrydstrup, T. *Chem. Commun.* **1999**, 343. Shabangi, M.; Flowers, R. A., II. *Tetrahedron Lett.* **1997**, 38, 1137–1140).

(10) One has to assume that the average association constant of Sm^{+3} to the dimer is similar to that of the radical anion, thereby maintaining a nearly constant concentration of Sm^{+3} .

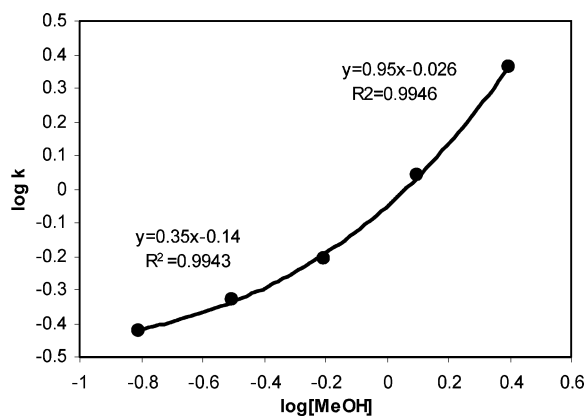


Figure 4. The dependence of the first-order rate constants of the second phase of the reaction of **DP** (12.5 mM) and SmI_2 (2.5 mM) on the concentration of MeOH.

Table 3. First-Order Rate Constant for the Reaction of **DP** (12.5 mM) with SmI_2 (2.5 mM) in the Presence of Varying Concentrations of MeOH

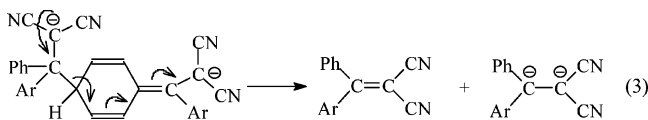
[MeOH] (M)	k_{obs} (s^{-1})
0.156	0.38
0.313	0.47
0.625	0.62
1.25	1.1
2.5	2.31

law for the disappearance of the dimer absorption (followed at 430 nm) is given in eq 2.

$$-\frac{d[\text{dimer}]}{2 dt} = k_{2\text{nd}}[\text{dimer}][\text{ROH}]^n, \quad n \approx 0.3-1 \quad (2)$$

Shown in Figure 4 and Table 3 (for **MA**, see Table S3) is the gradual change in the reaction order of MeOH from ca. 0.3 at low concentration to ca. 1 at higher concentration in the reaction of **DP**.

This may indicate the existence of two competing mechanisms: at low concentrations of MeOH, a mechanism where proton transfer takes place only after the rate-determining step (=zero order in MeOH), and at higher MeOH concentration, a mechanism where proton transfer takes place at the rate-determining step. A possible mechanism for the proton-donor-independent process is the cleavage of the dimer to the neutral reactant and its dianion (eq 3).



This indeed is a very slow step, and, therefore, in the absence of an appreciable amount of a proton donor, the reaction stretches over several hundred seconds. As the concentration of the proton donor increases, the protonation becomes the dominant path (see SPECFIT¹¹ simulation in the Supporting Information). As a result, the order in MeOH increases toward 1 and a kinetic H/D isotope effect is obtained ($k_{\text{H}}/k_{\text{D}} = 2.7$; $[\text{SmI}_2] = 2.5 \text{ mM}$; $[\text{DP}] = 12.5 \text{ mM}$ and $[\text{MeOH}] = 1.25 \text{ M}$).

(11) SPECFIT Global Analysis System (v. 2.11, Spectrum Software Associates).

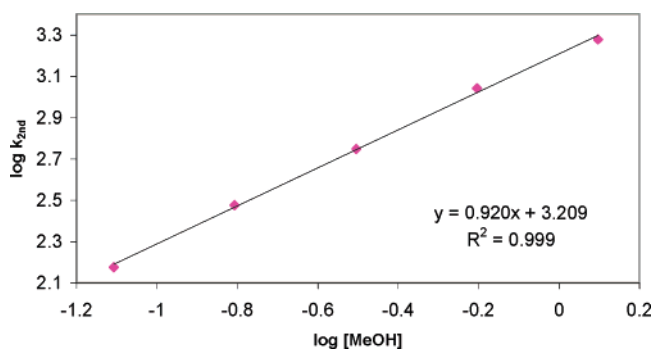


Figure 5. A plot of the log of the second-order reaction of **DA** (12.5 mM) with SmI_2 (2.5) versus the log of MeOH concentration.

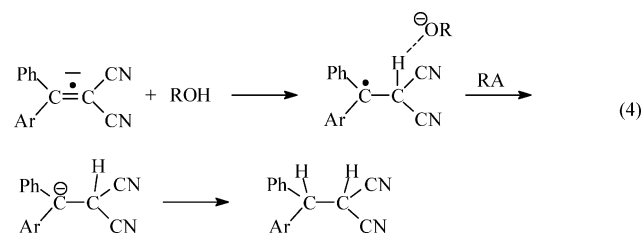
Table 4. Second-Order Rate Constant for the Reaction of **DA** (12.5 mM) with SmI_2 (2.5 mM) in the Presence of Varying Concentrations of MeOH

[MeOH] (M)	k_{obs} ($\text{M}^{-1} \text{ s}^{-1}$)
1.25	1900
0.625	1100
0.313	560
0.156	300
0.078	150

Ethylene glycol is known to enhance reductions by SmI_2 much more than the other alcohols.¹² Using ethylene glycol concentrations much smaller than MeOH (0.01–0.05 M) enhanced the second phase to such an extent that only the first phase was observed.

Disubstituted Substrates. The disubstituted substrates (**DA**, **DM**, and **DCI**, kinetic data were gathered for **DA**, while **DM** and **DCI** were only qualitatively examined) reacting with SmI_2 show the same absorption bands around 430 and 550 nm as **DP** and **MA**. Yet, only one phase is observed, the duration of which is in the order of several hundred seconds (see Figures S2, S3). The absorption of the radical anion decreases monotonically, retaining its shape all along. The reactions are second order in the radical anion, and their rates are largely enhanced by added MeOH. The reactions are first order in MeOH (Table 4, Figure 5) with no kinetic H/D isotope effect ($k_{\text{H}}/k_{\text{D}} = 1.13 \pm 0.15$) for concentrations of MeOH between 0.125 and 2.0 M.

The most plausible mechanism for the reaction of the disubstituted substrates is a reversible protonation of the radical anion forming an internal return complex with a rate-determining electron transfer from another radical anion (eq 4).



The absence of a kinetic H/D isotope effect is due to the reversible proton transfer within the internal return complex.¹³ Thus, when the two para positions are taken by substituents that block the dimerization path, the traditional Birch sequence

(12) Dahlen, A.; Hilmersson, G. *Tetrahedron Lett.* **2001**, *42*, 5565–5569.

of electron–proton–electron–proton transfer takes place. However, this process is much slower than the detour mechanism.

How frequently would a detour mechanism, similar to the one above, be encountered? Our analysis suggests that it may be encountered in many cases of olefin reduction by SmI_2 , although not in carbonyl reductions. The major reason for the detour mechanism is the sluggishness of the protonation of the radical anion relative to the coupling (dimerization) route. Let us first compare protonation of a negatively charged carbon with that of a negatively charged oxygen. The alcohol derived from the carbonyl compound will, in most cases, be of acidity similar to that of the protonating alcohol. According to the Eigen mechanism,¹⁴ proton transfer between two heteroatoms has a negligible intrinsic barrier, and the protonation rate of the alkoxide will be nearly diffusion-controlled. The situation is entirely different with olefins. For an olefin to accept an electron from SmI_2 , its corresponding anion has to be relatively stable. We have found, for example, that activation by a phenyl and a cyano group, as in α -cyanostilbene, is insufficient to promote a reaction. Thus, the olefin should be activated by strong electron-attracting groups such as two cyano groups as in the present case. This will lead to anions more resistant to protonation. In the absence of $\text{p}K_a$ values in THF, we will use the DMSO values determined by Bordwell et al.¹⁵ In DMSO, the $\text{p}K_a$ of malononitrile (the model activating group in the present study) is 11, and that of MeOH is 29. Thus, there is a huge thermodynamic barrier for protonation on the corresponding carbanion. In addition, it is well known that protonation on carbon has a significant intrinsic barrier that is absent in proton transfer between heteroatoms.¹⁶ As a consequence of the kinetic and the thermodynamic barriers, at the closed shell level, protonation on carbanions will be many orders of magnitude slower than that on alkoxide. Turning now to the open shell species, the radical anions, a number of effects must be considered. We note that a radical at the α position to oxygen increases its acidity by about 5 $\text{p}K_a$ units.¹⁷ A similar effect is expected for the double bond system. Therefore, the reactivity gap between the protonation on the carbonyl and the olefin-based radical anions will be retained. Finally, we must also consider the effect of the interaction of the Sm^{+3} cation with the various negatively charged species. The trivalent samarium is known to be very hard, while the delocalized radical anions are relatively soft. Therefore, they will be somewhat stabilized by Sm^{+3} as a gegenion slowing down the protonation rate. On the other hand, the interaction with the Sm^{+3} cation may increase the acidity of the proton donor. Brown¹⁸ has shown that complexation to Eu^{+3} increases the acidity of MeOH by ca. 10 $\text{p}K_a$ units. Assuming a similar effect with Sm^{+3} , this will reduce the $\text{p}K_a$ of MeOH to 19. This will bring again the protonation on the radical anion of the carbonyl compound to the vicinity

of the diffusion-controlled rate. However, the protonation rate on the olefinic radical anion will be many orders of magnitude below that value.

In conclusion, it is reasonable to assume that the effect of placing an odd electron at a position α to the negative charge, on the one hand, and the interaction of the Sm^{+3} with the radical anions, on the other, are similar although not necessarily identical in both cases. Therefore, the aforementioned thermodynamic and kinetic barriers are the origin of the vast reactivity gap, which greatly favors protonation on the radical anion of carbonyl over that of an olefin. This sluggishness in protonation on olefinic radical anions diverts them from reacting in the normal Birch mechanism to the alternative detour mechanism.

It should be pointed out that the reduction of olefins of lower activity (such as the α -cyanostilbene mentioned above) could be achieved by using additives such as HMPA¹⁹ that enhance the electron-transfer rate. In this case, the radical anion formed may be basic enough to undergo rapid protonation. In addition, using different solvents may decrease the acidity gap mentioned above. SmI_2 was recently shown to be stable in water.²¹ Using water as an example is, therefore, very instructive in this case. In water, the $\text{p}K_a$ of malononitrile (which serves as a model for the activating group in the present system) remains 11.²⁰ Yet, that of MeOH is reduced from 29 in DMSO to 16, and that of water itself is 15.5. It is thus possible that a large enough concentration of additives such as water or alcohol, which were found to increase the reaction rates, may provide,^{2k,j} in addition to their other enhancing effects, the micro environment needed for such proton transfer.

Experimental Section

THF was refluxed over Na wire with benzophenone and distilled under argon. Water content was determined (K.F. Coulometer 652) to be 20 ppm. SmI_2 was diluted as needed from a 0.1 M commercial THF solution. The concentration of the SmI_2 solution was spectroscopically determined ($\lambda = 615 \text{ nm}$; $\epsilon = 635$). All of the 1,1-diaryl-2,2-dicyanoethylenes used in the kinetic studies are known compounds.^{3a,21,22}

The kinetics of the reactions was followed using a stopped flow spectrophotometer (Hi-Tech SF-61DX2) in a glove box under nitrogen atmosphere. The reactions were monitored at 430 and/or 550 nm. In cases where a proton donor was used, the proton donor was mixed with the substrate solution. The water content in the THF solutions was determined (ca. 20 ppm) using a K.F. Coulometer-652. Because of the variable water content, all rate constants reported here were determined within a series of measurements performed on the same day using the same stock solutions. At the end of each series, the first measurement was repeated to ensure reproducibility within a set. The deviation did not usually exceed 8%. The kinetics were analyzed using KinetAsyst (v. 2.2 Hi-Tech Ltd.) and the SPECFIT Global Analysis System (v. 2.11, Spectrum Software Associates).¹¹

Supporting Information Available: Figure S1: Diode array spectra for the reaction of **DP** with SmI_2 . Short phase, 0.4 s and long phase, 200 s. Figure S2: Reaction of **DA** (25 mM) with SmI_2 (1.25 mM). Figure S3: Reaction of **DA** (25 mM) with SmI_2 (6 mM); ethylene glycol (25 mM). Table S1: Effect of variable concentrations of $[\text{SmI}_2]_0$ on the second-order rate constant of **MA** (25 mM). Table S2: Effect of the added Sm^{+3} on the second-order rate constants of the first phase for the

- (13) (a) Cram, D. J.; Kingsbury, C. A.; Rickborn, B. *J. Am. Chem. Soc.* **1961**, *83*, 3688–3696. (b) Hine, J.; Philips, C.; Maxwell, J. I. *J. Org. Chem.* **1970**, *35*, 3943–3945. (c) Streitwieser, A. J., Jr.; Owens, P. H.; Sonnichsen, G.; Smith, W. K.; Ziegler, G. R.; Niemeyer, H. M.; Kruger, T. L. *J. Am. Chem. Soc.* **1973**, *95*, 4254–4257. (d) Macciantelli, D.; Seconi, G.; Eaborn, C. *J. Chem. Soc., Perkin Trans. 2* **1978**, 834–838. (e) Thibblin, A.; Jencks, W. P. *J. Am. Chem. Soc.* **1979**, *101*, 4963–4973. (f) Fishbein, J. C.; Jencks, W. P. *J. Am. Chem. Soc.* **1988**, *110*, 5087–5095.
- (14) Eigen, M. *Angew. Chem., Int. Ed. Engl.* **1964**, *3*, 1.
- (15) Bordwell, F. G. *Acc. Chem. Res.* **1988**, *21*, 456–463.
- (16) Bell, R. P. *The Proton in Chemistry*; Chapman and Hall: London, 1973; p 131.
- (17) Hayon, E.; Simic, M. *Acc. Chem. Res.* **1974**, *7*, 114.
- (18) Neverov, A. A.; Gibson, G.; Brown, R. S. *Inorg. Chem.* **2003**, *42*, 228–234.

- (19) Inanaga, J.; Ishikawa, M.; Yamaguchi, M. *Chem. Lett.* **1987**, 1485–1486.
- (20) Pearson, R. G.; Dillon, R. L. *J. Am. Chem. Soc.* **1953**, *75*, 2439–2443.
- (21) Bruice, T. C.; Bradbury, W. C. *J. Org. Chem.* **1966**, *28*, 3403.
- (22) Charles, G. *Bull. Soc. Chim. Fr.* **1963**, 1559.

reaction of **MA**. Table S3: First-order rate constant for the reaction of **MA** in the presence of varying concentrations of MeOH. A SPECFIT simulation was run from the second phase of **DP**. Complete ref 6. Archive file of the B3LYP/6-31+G*

calculation of the radical anion of **DP**. This material is available free of charge via the Internet at <http://pubs.acs.org>.

JA0686662